# UNIFORM A PRIORI ESTIMATES FOR DISCRETE SOLUTION OF NONLINEAR TENSOR DIFFUSION EQUATION IN IMAGE PROCESSING

OLGA DRBLÍKOVÁ

This paper concerns with the finite volume scheme for nonlinear tensor diffusion in image processing. First we provide some basic information on this type of diffusion including a construction of its diffusion tensor. Then we derive a semi-implicit scheme with the help of so-called diamond-cell method (see Coirier [2] and Coirier, Powell [3]). Further, we prove existence and uniqueness of a discrete solution given by our scheme. The proof is based on a gradient bound in the tangential direction by a gradient in normal direction. Moreover, the proofs of $L^2(\Omega)$ – a priori estimates for our discrete solution are given. Finally we present our computational results.

*Keywords:* finite volume method, diamond-cell method, image processing, nonlinear parabolic equation, tensor diffusion

*AMS Subject Classification:* 35K60, 94A08, 74S10

## 1. INTRODUCTION

The effort to gain processed image quicker and by a less computationally expensive way leads to inventions of new diffusion models and also to their improvements. One of them was introduced by Weickert (see, e. g., [10]) in the following form

$$\frac{\partial u}{\partial t} - \nabla \cdot (D \nabla u) \quad = \quad 0, \qquad \text{in } Q_T \equiv I \times \Omega, \tag{1}$$

$$u(x,0) \quad = \quad u_0(x), \quad \text{in } \Omega, \tag{2}$$

$$\langle D \nabla u, n \rangle \quad = \quad 0, \qquad \text{on } I \times \partial\Omega, \tag{3}$$

where $u$ denotes an intensity of greylevel image and $D$ is a matrix depending on the eigenvalues and on the eigenvectors of the so-called (regularized) structure tensor $J = \nabla u (\nabla u)^T$ (for details see next section). This modification is useful in any situation, where strong smoothing in one direction and low smoothing in the perpendicular direction are desirable. Owing to this property, tensor anisotropic diffusion has been applied mainly for images with interrupted coherence of structures.

We derive our numerical scheme for this diffusion model by finite volume method. We choose this modern discretization technique since it is well suited for a numerical

solution of conservation laws. It has been successfully applied in image processing, e. g., for solving the Perona–Malik equation [9] or curvature driven level set equation [8].

## 2. DERIVATION OF DIFFUSION TENSOR

### 2.1. Analyzing coherent structures

In order to enhance a coherence of structures, we need a reliable tool for analyzing coherent structures.

A very simple structure descriptor is given, e. g., by the properties of $\nabla u_{\tilde{t}}$, where

$$u_{\tilde{t}}(x, t) \quad = \quad (G_{\tilde{t}} * u(\cdot, t))(x), \qquad (\tilde{t} > 0). \tag{4}$$

Let us note that $\tilde{t}$ of Gaussian kernel $G_{\tilde{t}}$ denotes the noise scale (the edge detector ignore details smaller than $O(\tilde{t})$). We can use, e. g., absolute value of $\nabla u_{\tilde{t}}$ for detecting edges in some images (see [1]) but for images with line structures this descriptor is not useful. We know that high fluctuations remain for small $\tilde{t}$, while larger $\tilde{t}$ leads to entirely useless results. This is due to fact that for larger $\tilde{t}$ neighboring gradients with same orientation but opposite sign cancel each other. One way how to gain the structure descriptor invariant under sign changes is to replace $\nabla u_{\tilde{t}}$ by its tensor product. Then we again average it by applying other convolution with Gaussian $G_\rho$

$$J_\rho(\nabla u_{\tilde{t}}) = G_\rho * (\nabla u_{\tilde{t}} \nabla u_{\tilde{t}}^T), \qquad (\rho \geq 0) \tag{5}$$

where $\rho$ denotes the integration scale, which reflects the characteristic size of the texture and in the most cases, it is large in comparison to the noise scale $\tilde{t}$. In computer vision community the matrix

$$J_\rho = \begin{pmatrix} a & b \\ b & c \end{pmatrix}$$

is well-known as structure tensor. This matrix $J_\rho$ is symmetric and positive semi-definite and its eigenvalues are given as follows

$$\mu_{1,2} = \frac{1}{2}\left(a + c \pm \sqrt{(a-c)^2 + 4b^2}\right), \qquad \mu_1 \geq \mu_2. \tag{6}$$

The eigenvalues describe the average contrast in the eigendirections $\tilde{\mathbf{v}}$ and $\tilde{\mathbf{w}}$.

The corresponding orthonormal set of eigenvectors $(\tilde{\mathbf{v}}, \tilde{\mathbf{w}})$ to eigenvalues $(\mu_1, \mu_2)$ is given by

$$\tilde{\mathbf{v}} = (v_1, v_2), \qquad \tilde{\mathbf{w}} = (w_1, w_2), \tag{7}$$
$$v_1 = 2b, \qquad v_2 = c - a + \sqrt{(a-c)^2 + 4b^2},$$
$$\tilde{\mathbf{w}} \perp \tilde{\mathbf{v}}, \qquad w_1 = -v_2, \qquad w_2 = v_1.$$

The orientation of the eigenvector $w$, which corresponds to the smaller eigenvalue $\mu_2$ is called coherence orientation. This orientation has the lowest fluctuations.

## 2.2.  Coherence-enhancing anisotropic diffusion

Since we have a tool for analyzing coherence, we draw our goals to enhance the image coherence. One of possibilities, how to do it, can be done by embedding the structure tensor analysis into a nonlinear diffusion filter.

For enhancing coherence, the diffusion tensor $D$ must steer a filtering process such that diffusion is strong mainly along the coherence direction $\tilde{\mathbf{w}}$ and it increases with the coherence $(\mu_1 - \mu_2)^2$. To obtain it, we require that $D$ must possess the same eigenvectors $\tilde{\mathbf{w}}$ and $\tilde{\mathbf{w}}$ as the structure tensor $J_\rho(\nabla u_{\tilde{t}})$ and we choose the eigenvalues of $D$ as

$$
\begin{aligned}
\kappa_1 &= \alpha, \quad \alpha \in (0,1),\ \alpha \ll 1, \\
\kappa_2 &= \begin{cases} \alpha, & \text{if } \mu_1 = \mu_2, \\ \alpha + (1-\alpha)\exp\left(\frac{-C}{(\mu_1 - \mu_2)^2}\right), & C > 0 \quad \text{else.} \end{cases}
\end{aligned}
$$

The diffusion tensor $D$ has a form

$$
D = ABA^{-1} = \begin{pmatrix} \lambda & \beta \\ \beta & \nu \end{pmatrix}, \tag{8}
$$

$$
\text{where} \quad A = \begin{pmatrix} v_1 & -v_2 \\ v_2 & v_1 \end{pmatrix} \quad \text{and} \quad B = \begin{pmatrix} \kappa_1 & 0 \\ 0 & \kappa_2 \end{pmatrix}.
$$

Due to the convolutions in (4) and (5), the elements of matrix $D$ are $C^1$ functions.

## 3.  FINITE–VOLUME SCHEME FOR TENSOR ANISOTROPIC DIFFUSION IN IMAGE PROCESSING

The aim of this section is to prove the existence of a unique discrete solution for the model $(1)-(3)$ which satisfies the semi-implicit finite volume scheme obtained with the help of co-volume mesh. Let us consider a rectangular image domain $\Omega = (0, n_1 h) \times (0, n_2 h)$, $h$ is a pixel size and let the image $u(x)$ be represented by a bounded mapping $u : \Omega \to R$. Our image is represented by $n_1 \times n_2$ pixels (finite volumes) such that it looks as mesh with $n_1$ rows and $n_2$ columns. We consider it in a scaling (time) interval $I = [0, T]$. Let $0 = t_0 \le t_1 \le \cdots \le t_{N_{\max}} = T$ denotes the time discretization with $t_n = t_{n-1} + k$, where $k$ is the time (scale) step. For $n = 0, \ldots, N_{\max}$ we will look for $u^n$ an approximation of solution at time $t_n$.

We integrate equation (1) over finite volume $K$, provide a semi-implicit in time discretization and use a divergence theorem to get

$$
\frac{u_K^n - u_K^{n-1}}{k} m(K) - \sum_{\sigma \in \mathcal{E}_K} \int_\sigma D^{n-1} \nabla u^n \cdot \tilde{\mathbf{n}}_{K,\sigma}\, \mathrm{d}s = 0, \tag{9}
$$

where $u_K^n$, $K \in \mathcal{T}_h$ represents the mean value of $u^n$ on $K$, $m(K)$ is the measure of the finite volume $K$ with boundary $\partial K$, $\sigma_{KL} = K \cap L = K|L$ is an edge of the finite volume $K$, where $L \in \mathcal{T}_h$ is an adjacent finite volume to $K$ such that $m(K \cap L) \neq 0$. Let us note that only due to simpler notation, we will write in the sequel $\sigma$ instead

of $\sigma_{KL}$. $\mathcal{E}_K$ is a subset of $\mathcal{E}$ such that $\partial K = \bigcup_{\sigma \in \mathcal{E}_K} \sigma$, $\mathcal{E} = \bigcup_{K \in \mathcal{T}_h} \mathcal{E}_K$, where $\mathcal{T}_h$ is admissible finite volume mesh (see [6]). $\Upsilon$ is the set of pairs of adjacent finite volumes, defined by $\Upsilon = \{(K, L) \in \mathcal{T}_h^2, K \neq L, m(K|L) \neq 0\}$. We will denote $D_\sigma^{n-1}$ as mean value of $D^{n-1} \equiv D(u^{n-1})$ on $\sigma$, that is $D_\sigma^{n-1} = \frac{1}{m(\sigma)} \int_\sigma D^{n-1} \, dx$, where $m(\sigma)$ is the measure of edge $\sigma$, and $\tilde{\mathbf{n}}_{K,\sigma}$ is the normal unit vector to $\sigma$ outward to $K$. Let us define the discrete solution by

$$u_{h,k}(x,t) = \sum_{n=0}^{N_{\max}} \sum_{K \in \mathcal{T}_h} u_K^n \chi\{x \in K\}\chi\{t_{n-1} < t \leq t_n\}, \tag{10}$$

where the function $\chi(A)$ is defined as

$$\chi_{\{A\}} = \begin{cases} 1, & \text{if } A \text{ is true,} \\ 0, & \text{elsewhere.} \end{cases}$$

Due to theoretical reasons we have to extend such defined $u_{h,k}$ outside $\Omega$. To that goal we defined the set

$$\Omega_{\bar{t}} = \Omega \cup B_{\bar{t}}(x), \quad x \in \partial\Omega, \tag{11}$$

where $B_{\bar{t}}(x)$ is a ball centered at $x$ with radius $\tilde{t}$ and extension $\tilde{u}_{h,k}$ in the following way: outside $\Omega_{\bar{t}}$, $\tilde{u}_{h,k} \equiv 0$. In $\Omega_{\bar{t}} - \Omega$ we define $\tilde{u}_{h,k}$ by mirror reflexion and periodization through sides of $\Omega$ (rectangular domain), where the number of such mirror reflexions depends on the size of $\tilde{t}$ (see [7]). In order to get an approximation of equation (9) we write it in the form

$$\frac{u_K^n - u_K^{n-1}}{k} - \frac{1}{m(K)} \sum_{\sigma \in \mathcal{E}_K} \phi_\sigma^n(u_{h,k}^n) m(\sigma) = 0, \tag{12}$$

where $\phi_\sigma^n(u_{h,k}^n)$ denotes an approximation of the exact flux $\frac{1}{m(\sigma)} \int_\sigma D_\sigma^{n-1} \nabla u^n \cdot \tilde{\mathbf{n}}_{K,\sigma} \, ds$ and $u_{h,k}^n(x) = \sum_{K \in \mathcal{T}_h} u_K^n \chi\{x \in K\}$.

One possibility how to construct $\phi_\sigma^n(u_{h,k}^n)$ is obtained with the help of co-volume mesh. The specific name (diamond-cell) of this method (see [2] and [3]) is due to the choice of co-volume as a diamond-shaped polygon. The co-volume $\chi_\sigma$ associated to $\sigma$ is constructed around each edge by joining all four co-volume vertices (i. e. endpoints of this edge and midpoints of finite volumes which are common to this edge) (see Figure 1).

We denote the endpoints of an edge $\bar{\sigma} \subset \partial\chi_\sigma$ by $N_1(\bar{\sigma})$ and $N_2(\bar{\sigma})$ and $\tilde{\mathbf{n}}_{\chi_\sigma, \bar{\sigma}}$ is the normal unit vector to $\bar{\sigma}$ outward to $\chi_\sigma$. In order to have an approximation of the diffusion flux, we first derive, using divergence theorem, an approximation of the averaged gradient on $\sigma$

$$\frac{1}{m(\chi_\sigma)} \int_{\chi_\sigma} \nabla u^n \, dx = \frac{1}{m(\chi_\sigma)} \int_{\partial\chi_\sigma} u^n \tilde{\mathbf{n}}_{\chi_\sigma, \bar{\sigma}} \, ds$$

and then we denote it by

$$p_\sigma^n = \frac{1}{m(\chi_\sigma)} \sum_{\bar{\sigma} \in \partial\chi_\sigma} \frac{1}{2} \left( u_{N_1(\bar{\sigma})}^n + u_{N_2(\bar{\sigma})}^n \right) m(\bar{\sigma}) \tilde{\mathbf{n}}_{\chi_\sigma, \bar{\sigma}}.$$
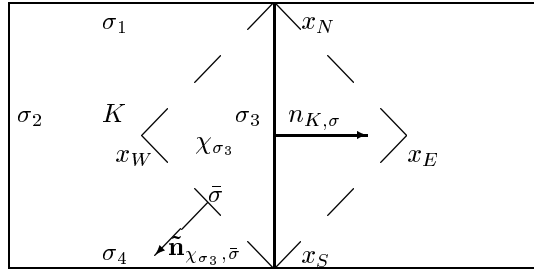
**Fig. 1.** A detail of a mesh – a finite volume $K$, its boundaries $\sigma_i$, $i = 1, 2, 3, 4$ and co-volume $\chi_{\sigma_3}$ corresponding to $\sigma_3$.

The value at the centres $x_E$ and $x_W$ are $u_E$ and $u_W$ while the values at the vertices $x_N$ and $x_S$ are computed as the arithmetic mean of values on finite volumes which are common to this vertex (for general nonuniform meshes see [2]).

Since our mesh is uniform squared, for simplification, we can use the following relations: $m(\chi_\sigma) = \frac{h^2}{2}$, $m(\bar{\sigma}) = \frac{\sqrt{2}}{2}h$ and after a short calculation we are ready to write

$$p_\sigma^n = \frac{u_E^n - u_W^n}{h}\tilde{\mathbf{n}}_{K,\sigma} + \frac{u_N^n - u_S^n}{h}\tilde{\mathbf{t}}_{K,\sigma}, \tag{13}$$

where $\tilde{\mathbf{t}}_{K,\sigma}$ is a unit vector parallel to $\sigma$ such that $(x_N - x_S) \cdot \tilde{\mathbf{t}}_{K,\sigma} > 0$. Although such $u_N^n$, $u_W^n$, $u_E^n$ and $u_S^n$ correspond to particular edge $\sigma$, we should denote them by $u_{N_\sigma}^n$, $u_{W_\sigma}^n$, $u_{E_\sigma}^n$ and $u_{S_\sigma}^n$, we use those simpler notations. Replacing the exact gradient $\nabla u^n$ by the numerical gradient $p_\sigma^n$ we get the numerical flux in the form

$$\phi_\sigma^n(u_{h,k}^n) = \frac{1}{m(\sigma)} \int_\sigma D^{n-1} p_\sigma^n \cdot \tilde{\mathbf{n}}_{K,\sigma}\, \mathrm{d}s = D_\sigma p_\sigma^n \cdot \tilde{\mathbf{n}}_{K,\sigma}, \tag{14}$$

where

$$D_\sigma = \frac{1}{m(\sigma)} \int_\sigma D^{n-1}\, \mathrm{d}s = \begin{pmatrix} \bar{\lambda}_\sigma & \bar{\beta}_\sigma \\ \bar{\beta}_\sigma & \bar{\nu}_\sigma \end{pmatrix}$$

in the basis $(\tilde{\mathbf{n}}_{K,\sigma}, \tilde{\mathbf{t}}_{K,\sigma})$. It means, if

$$D = \begin{pmatrix} \lambda & \beta \\ \beta & \nu \end{pmatrix} \qquad \text{then} \qquad D_{\sigma_2} = D_{\sigma_3} = \begin{pmatrix} \lambda_\sigma & \beta_\sigma \\ \beta_\sigma & \nu_\sigma \end{pmatrix},$$

i. e. $\bar{\lambda}_\sigma = \lambda_\sigma$, $\bar{\beta}_\sigma = \beta_\sigma$, $\bar{\nu}_\sigma = \nu_\sigma$. On the other hand,

$$D_{\sigma_1} = D_{\sigma_4} = \begin{pmatrix} \nu_\sigma & -\beta_\sigma \\ -\beta_\sigma & \lambda_\sigma \end{pmatrix},$$

i. e. $\bar{\lambda}_\sigma = \nu_\sigma$, $\bar{\beta}_\sigma = -\beta_\sigma$, $\bar{\nu}_\sigma = \lambda_\sigma$, where $\lambda_\sigma = \frac{1}{m(\sigma)} \int_\sigma \lambda^{n-1}\, \mathrm{d}s$ and $\beta_\sigma$ and $\nu_\sigma$ correspondingly. Definition (14) can be also written in this form

$$\phi_\sigma^n(u_{h,k}^n) = \begin{pmatrix} \bar{\lambda}_\sigma & \bar{\beta}_\sigma \\ \bar{\beta}_\sigma & \bar{\nu}_\sigma \end{pmatrix} \begin{pmatrix} \dfrac{u_E^n - u_W^n}{h} \\ \dfrac{u_N^n - u_S^n}{h} \end{pmatrix} \begin{pmatrix} 1 \\ 0 \end{pmatrix} = \bar{\lambda}_\sigma \frac{u_E^n - u_W^n}{h} + \bar{\beta}_\sigma \frac{u_N^n - u_S^n}{h}, \tag{15}$$

since (13) in the basis $(\tilde{\mathbf{n}}_{K,\sigma}, \tilde{\mathbf{t}}_{K,\sigma})$ can be for each edge written as

$$p_\sigma^n = \begin{pmatrix} \dfrac{u_E^n - u_W^n}{h} \\ \dfrac{u_N^n - u_S^n}{h} \end{pmatrix} \tag{16}$$

and $\tilde{\mathbf{n}}_{K,\sigma}$ in the basis $(\tilde{\mathbf{n}}_{K,\sigma}, \tilde{\mathbf{t}}_{K,\sigma})$ is equal to $\begin{pmatrix} 1 & 0 \end{pmatrix}^T$ for all edges.

In order to prove existence and uniqueness of $u_K^n$, $K \in \mathcal{T}_h$, we estimate the expressions $u_N^n - u_S^n$ by means of $u_E^n - u_W^n$ for all edges $\sigma$ in the following form

$$\sum_{\sigma \in \mathcal{E}_{int}} \left( \frac{\bar{\beta}_\sigma}{\bar{\lambda}_\sigma} \right)^2 \left( \frac{u_N - u_S}{h} \right)^2 \bar{\lambda}_\sigma \leq \gamma \sum_{\sigma \in \mathcal{E}} \left( \frac{u_E - u_W}{h} \right)^2 \bar{\lambda}_\sigma, \tag{17}$$

where

$$0 \leq \gamma < 1, \quad \gamma = \max_{\sigma \in \mathcal{E}} \gamma_\sigma, \quad \gamma_\sigma = \frac{(\beta_\sigma)^2}{\lambda_\sigma \nu_\sigma}(1 + O(h)) \tag{18}$$

for $h$ sufficiently small (for details see [5]).

Let us now introduce the space of piecewise constant functions associated to our mesh and discrete $H^1$ norm for this space. This discrete norm will be used to obtain some estimates on the approximate solution given by a finite volume scheme.

**Definition 3.1.** Let $\Omega$ be an open bounded polygonal subset of $R^2$. We define $\mathcal{P}_0(\mathcal{T}_h)$ as the set of functions from $\Omega$ to $R$ which are constant over each finite volume of the mesh.

**Definition 3.2.** Let $\Omega$ be an open bounded polygonal subset of $R^2$. For $u \in \mathcal{P}_0(\mathcal{T}_h)$ we define

$$|u_{h,k}^n|_{1,\mathcal{T}_h} = \left( \sum_{(K,L) \in \Upsilon} \frac{(u_L - u_K)^2}{d_{K,L}} m(\sigma) \right)^{\frac{1}{2}}, \tag{19}$$

where $d_{K,L}$ is the Euclidean distance between $x_K$ and $x_L$.

Remark that (19) can be rewritten into the following form

$$|u_{h,k}^n|_{1,\mathcal{T}_h} = \left( 2 \sum_{\sigma \in \mathcal{E}} \left( \frac{u_E - u_W}{h} \right)^2 m(\chi_\sigma) \right)^{\frac{1}{2}} \tag{20}$$

for our uniform mesh. We can define discrete operator for $(1) - (3)$ by

$$\mathcal{L}_h(u_{h,k}^n) = u_K^n m(K) - k \sum_{\sigma \in \mathcal{E}_K} \phi_\sigma^n(u_{h,k}^n) m(\sigma), \tag{21}$$

such that $u_{h,k}^n$ is the solution in $\mathcal{P}_0(\mathcal{T}_h)$ of

$$\mathcal{L}_h(u_{h,k}^n) = f_{h,k}(u_{h,k}^{n-1}), \tag{22}$$

where $f_{h,k}(u_{h,k}^{n-1}) = u_K^{n-1}m(K)$ and $u_K^{n-1}$ is a value of the piecewise constant function $u_{h,k}^{n-1}$ in $K$. This equality is a linear system of $N$ equations with $N$ unknowns, namely $u_K^n$, $K \in \mathcal{T}_h$, where $N = card(K)$. Multiplying $\mathcal{L}_h(u_{h,k})$ by $u_K^n$, summing over $K$ and splitting into a part $A$ and $B$ leads to

$$\sum_{K \in \mathcal{T}_h} \mathcal{L}_h(u_{h,k}^n)u_K^n = A + B, \tag{23}$$

with

$$A = \sum_{K \in \mathcal{T}_h} (u_K^n)^2 m(K) = \|u_{h,k}^n\|_{L^2(\Omega)}^2, \tag{24}$$

$$B = k \sum_{K \in \mathcal{T}_h} u_K^n \sum_{\sigma \in \mathcal{E}_K} -\phi_\sigma^n(u_{h,k}^n)m(\sigma) = Q(u_{h,k}^n). \tag{25}$$

Then we bound $Q(u_{h,k}^n)$ as follows

$$Q(u_{h,k}^n) \geq \bar{\lambda}_{\min} \frac{1-\gamma}{2} \frac{k}{2} |u_{h,k}^n|_{1,\mathcal{T}_h}^2, \tag{26}$$

where $\bar{\lambda}_{\min} = \inf_{\sigma \in \mathcal{E}} \bar{\lambda}_\sigma \geq C > 0$. Subsequently, it yields

$$\sum_{K \in \mathcal{T}_h} \mathcal{L}_h(u_{h,k}^n)u_K^n \geq \alpha \left( |u_{h,k}^n|_{1,\mathcal{T}_h}^2 + \|u_{h,k}^n\|_{L^2(\Omega)}^2 \right) \tag{27}$$

with $\alpha = \min\left(\bar{\lambda}_{\min}(1-\gamma)\frac{k}{2}, 1\right)$, (for details of derivation of this inequality see [5]).

**Theorem 3.3.** For $h$ sufficiently small, there exists unique solution $u_{h,k}$ given by scheme (12) with (15).

P r o o f. Assume that $u_{h,k}$ satisfies the linear system (22) and let $f = 0$. Using (27) and (22) we get

$$\alpha \left( |u_{h,k}^n|_{1,\mathcal{T}_h}^2 + \|u_{h,k}^n\|_{L^2(\Omega)}^2 \right) \leq \sum_{K \in \mathcal{T}_h} \mathcal{L}_h(u_{h,k}^n)u_K^n = \sum_{K \in \mathcal{T}_h} f u_K^n = 0. \tag{28}$$

Due to relation (28), we know that $u_K^n = 0$, $\forall K \in \mathcal{T}_h$. It means that kernel of the linear transformation represented by the matrix of the system (22) contains only $\bar{0}$ vector, which implies that the matrix is regular. And thus it implies that there exists unique solution for any right hand side. $\square$

**Lemma 3.4.**   ($L^2(\Omega)$ – a priori estimates)  The scheme (12) with (15) leads to the following estimates.

There exists a positive constant $C$ which does not depend on $h, k$ such that

$$\max_{0 \leq n \leq N_{\max}} \sum_{K \in \mathcal{T}_h} (u_K^n)^2 \, m(K) \leq C, \tag{29}$$

$$\sum_{n=1}^{N_{\max}} k \sum_{(K,L) \in \Upsilon} \frac{(u_K^n - u_L^n)^2}{d_{K,L}} m(\sigma) \leq C, \tag{30}$$

$$\sum_{n=1}^{N_{\max}} \sum_{K \in \mathcal{T}_h} \left(u_K^n - u_K^{n-1}\right)^2 m(K) \leq C. \tag{31}$$

   P r o o f   o f   $L^2(\Omega)$ – a   p r i o r i   e s t i m a t e s.   The scheme (12) can be written as

$$(u_K^n - u_K^{n-1}) m(K) = k \sum_{\sigma \in \mathcal{E}_K} \phi_{\sigma_{KL}}^n (u_{h,k}^n) m(\sigma). \tag{32}$$

We multiply (32) by $u_K^n$, sum it over $K \in \mathcal{T}_h$ and use the property $(a-b)a = \frac{1}{2}a^2 - \frac{1}{2}b^2 + \frac{1}{2}(a-b)^2$ on the left side of (32) to obtain

$$\frac{1}{2} \sum_{K \in \mathcal{T}_h} (u_K^n)^2 m(K) - \frac{1}{2} \sum_{K \in \mathcal{T}_h} (u_K^{n-1})^2 m(K) + \frac{1}{2} \sum_{K \in \mathcal{T}_h} (u_K^n - u_K^{n-1})^2 m(K)$$

$$= k \sum_{K \in \mathcal{T}_h} \sum_{\sigma \in \mathcal{E}_K} u_K^n \phi_{\sigma_{KL}}^n (u_{h,k}^n) m(\sigma). \tag{33}$$

We can rearrange $\sum_{K \in \mathcal{T}_h} \sum_{\sigma \in \mathcal{E}_K}$ into $\sum_{\sigma_{KL} \in \mathcal{E}}$ and then we add a sum over $n = 1, \ldots, m < N_{\max}$ to get

$$\frac{1}{2} \sum_{K \in \mathcal{T}_h} (u_K^m)^2 m(K) + \frac{1}{2} \sum_{n=1}^m \sum_{K \in \mathcal{T}_h} (u_K^n - u_K^{n-1})^2 m(K)$$

$$- k \sum_{n=1}^m \sum_{\sigma_{KL} \in \mathcal{E}} u_K^n \phi_{\sigma_{KL}}^n (u_{h,k}^n) m(\sigma) = \frac{1}{2} \sum_{K \in \mathcal{T}_h} (u_K^0)^2 m(K). \tag{34}$$

And from it using (25) and (26) we have

$$\frac{1}{2} \sum_{K \in \mathcal{T}_h} (u_K^m)^2 m(K) + \frac{1}{2} \sum_{n=1}^m \sum_{K \in \mathcal{T}_h} (u_K^n - u_K^{n-1})^2 m(K)$$

$$+ \bar{\alpha} \sum_{n=1}^m k |u_{h,k}^n|_{1,\mathcal{T}_h}^2 \leq \frac{1}{2} \sum_{K \in \mathcal{T}_h} (u_K^0)^2 m(K) \tag{35}$$

with a positive constant $\bar{\alpha}$. Since $u_K^0 \in L^2(\Omega)$, the right hand side is bounded by a positive constant $C$. Using the first term of (35) we get the first $L^2(\Omega)$ – a priori estimate (29) and from the second term of (35) we have the third $L^2(\Omega)$ – a priori estimate (31). From strict positiveness of $\bar{\alpha}$ in the third term of (35) and from definition (19) we obtain the second $L^2(\Omega)$ – a priori estimate (30).   $\square$

### 4. NUMERICAL EXPERIMENTS

The aim of this section is to present behavior of the nonlinear tensor diffusion, using our scheme (12) with the numerical flux given by (15).

In these experiments we use spatial step $h = 0.01$, time step $k = 0.0001$, $C = 1$, $\alpha = 0.001$, $\tilde{t} = 0.00001$ and $\rho = 0.002$. The arising sparse linear systems are solved by Gauss–Seidel iterative method. For numerical implementation we use the programming language C.
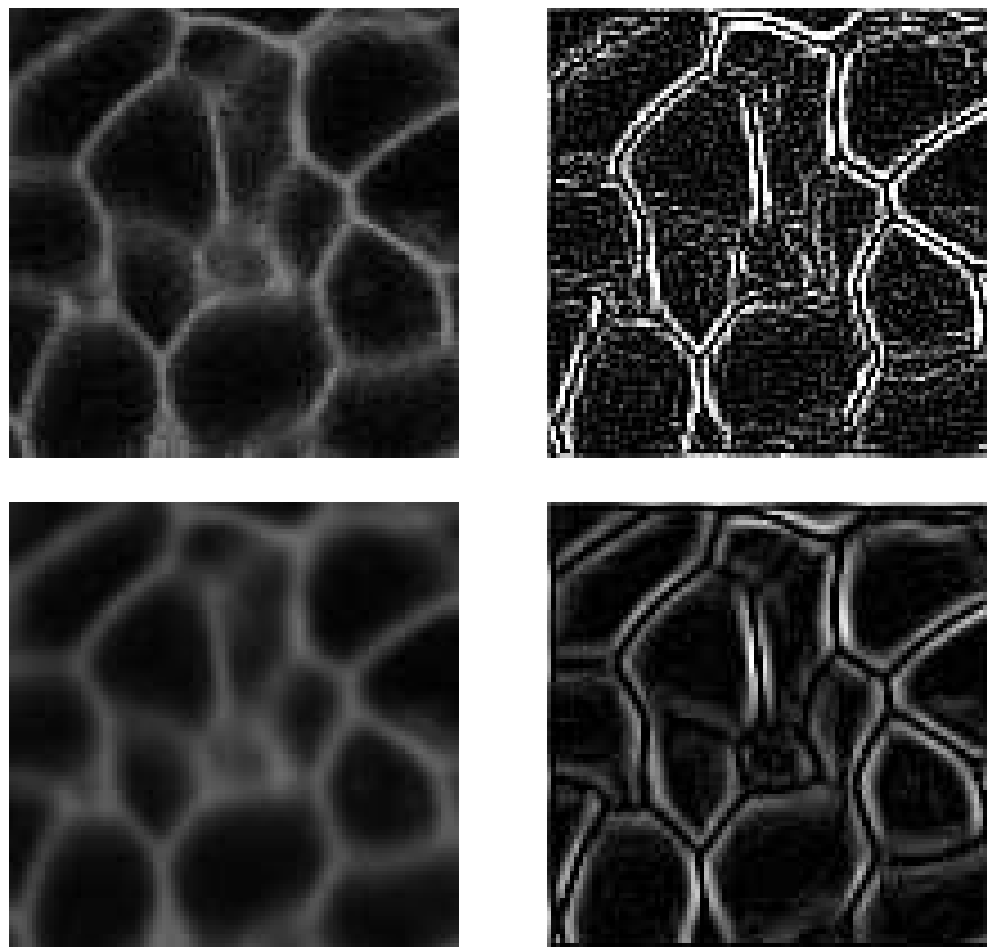


**Fig. 2.** Cell membranes. The image size is $100 \times 100$ pixels. Top (left): original image. Top (right): edge detection for the original image. Bottom (left): image after 4 filtering steps. Bottom (right): edge detection for the image after 4 steps.

The images used for our computational experiments were obtained by multi-photon laser scanning microscopy. They are chosen from series of images which
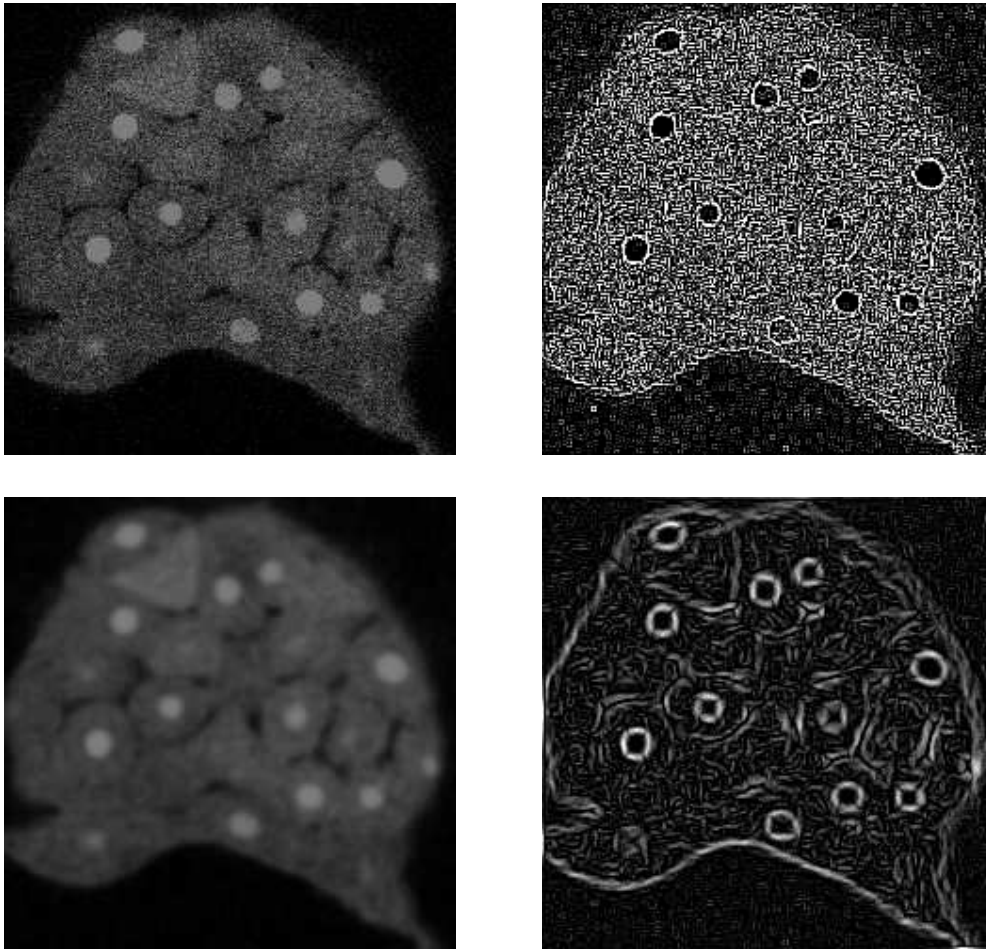
depict cells of zebra-fish embryogenesis.



**Fig. 3.** Cells with nuclei and membranes as well. The image size is 240 × 240 pixels. Top (left): original image. Top (right): edge detection for the original image. Bottom (left): image after 5 filtering steps. Bottom (right): edge detection for the image after 5 steps.

Our experiments are presented in two examples. Figure 2 shows cell membranes of the embryo while in Figure 3 cell membranes and nuclei of the embryo are illustrated. Both figures consist of four sub-figures. For each of these figures, we depict an original noisy image at the top (left), a smoothed image at the bottom (left), an edge detection which corresponds to the original image at the top (right) and an edge detection which corresponds to the filtered image at the bottom (right). We use Sobel method of edge detection.

We demonstrate an effect of smoothing and emphasizing of line structures in

these figures. Even if filtered images (Figure 2−3 bottom (left))) are more blurred compared with original images (Figure 2−3 top (left)), one can observe that line structures (boundaries of membranes and nuclei) (Figure 2−3 bottom (right)) are clearly detected compared with the original images (Figure 2−3 top (right)). This enhancement of edge detection is useful for subsequent image processing, e. g., segmentation. Human eye can see boundaries of membranes and nuclei of the original images and filtered ones. However, the computer using edge detection "is not able to recognize" some boundaries of the original image, e. g., membranes of small cell in the middle of the image and its left and right neighboring cells as well (see Figure 2 top). On the other hand, the computer "can easy detect" these cells using edge detection of the filtered image (see Figure 2 bottom (right)). The difference between edge detection of the original and filtered images is even more expressive in Figure 3. One is able to recognize only boundaries of cell nuclei in the edge detection of the original image (see Figure 3 top (right)) while after filtering we can also see boundaries of cell in the edge detection (see Figure 3 bottom (right)).

The satisfactory results were obtained after few time steps, so the denoising method is really fast. In the presented experiments we do not observe any stability problems which is a usual drawback of explicit schemes, (see [11]).

REFERENCES

[1]  F. Catté, P. L. Lions, J. M. Morel, and T. Coll: Image selective smoothing and edge detection by nonlinear diffusion. SIAM J. Numer. Anal. *129* (1991), 182–193.

[2]  W. J. Coirier: An a Adaptively-Refined, Cartesian, Cell-Based Scheme for the Euler and Navier-Stokes Equations. PhD Thesis, Michigan Univ. NASA Lewis Research Center, 1994.

[3]  W. J. Coirier and K. G. Powell: A cartesian, cell-based approach for adaptive-refined solutions of the Euler and Navier–Stokes equations. AIAA 1995.

[4]  Y. Coudiere, J. P. Vila, and P. Villedieu: Convergence rate of a finite volume scheme for a two-dimensional convection-diffusion problem. M2AN Math. Model. Numer. Anal. *33* (1999), 493–516.

[5]  O. Drblíková: Finite volume schemes for tensor anisotropic diffusion in image processing. In: Proc. MAGIA 2005, STU Bratislava 2005, pp. 7–18. (www.math.sk/drblikov)

[6]  R. Eymard, T. Gallouët, and R. Herbin: Finite Volume Methods. In: Handbook for Numerical Analysis, Vol. 7 (Ph. Ciarlet, J. L. Lions, eds.), Elsevier, Amsterdam 2000.

[7]  F. Guichard and J. M. Morel: Image Analysis and P.D.E.s. IPAM GBM Tutorials, 2001.

[8]  A. Handlovičová, K. Mikula, and F. Sgallari: Semi-implicit complementary volume scheme for solving level set like equations in image processing and curve evolution. Numer. Math. *93* (2003), 675–695.

[9] K. Mikula and N. Ramarosy: Semi-implicit finite volume scheme for solving nonlinear diffusion equations in image processing. Numer. Math. *89* (2001), 561–590.

[10] J. Weickert: Coherence-enhancing diffusion filtering. Internat. J. Comput. Vision *31* (1999), 111–127.

[11] J. Weickert and H. Scharr: A scheme for coherence-enhancing diffusion filtering with optimized rotation invariance. J. Visual Comm. and Image Repres. *13* (2002), 1–2, 103–118.

*Olga Drblíková, Department of Mathematics and Descriptive Geometry, Faculty of Civil Engineering, Slovak University of Technology in Bratislava, Radlinského 11, 813 68 Bratislava. Slovak Republic.*
*e-mails: drblikov@math.sk*